GLIA 48:311–326 (2004)

Voltage-Dependent Potassium Currents in Hypertrophied Rat Astrocytes After a Cortical Stab Wound

MIROSLAVA ANDĚROVÁ,[1,2,3]* TATIANA ANTONOVA,[1] DAVID PETŘÍK,[1] HELENA NEPRAŠOVÁ,[1,3] ALEXANDR CHVÁTAL,[1,2,3] AND EVA SYKOVÁ[1,2,3]

[1]*Department of Neuroscience, Institute of Experimental Medicine, Academy of Sciences of the Czech Republic, Prague, Czech Republic*

[2]*Department of Neuroscience, Charles University, Second Medical Faculty, Prague, Czech Republic*

[3]*Center for Cell Therapy and Tissue Repair, Charles University, Prague, Czech Republic*

KEY WORDS CNS injury, astrogliosis, GFAP, extracellular potassium, patch-clamp

ABSTRACT Changes in the membrane properties of reactive astrocytes in gliotic cortex induced by a stab wound were studied in brain slices of 21–28-day-old rats, using the patch-clamp technique and were correlated with changes in resting extracellular K^+ concentration ($[K^+]_e$) measured in vivo using K^+-selective microelectrodes. Based on K^+ current expression, three types of astrocytes were identified in gliotic cortex: A1 astrocytes expressing a time- and voltage-independent K^+ current component and additional inwardly rectifying K^+ currents (K_{IR}); A2 astrocytes expressing a time- and voltage-independent K^+ current component and additional delayed outwardly rectifying K^+ currents (K_{DR}); and complex astrocytes expressing K_{DR}, K_{IR}, and A-type K^+ (K_A) currents and Na^+ currents (I_{Na}). Nestin/bromodeoxyuridine (BrdU)-negative A1 astrocytes were found further than ~100 μm from the stab wound and showed an upregulation of K_{IR} currents within the first day post-injury (PI), correlating with an increased resting $[K^+]_e$. Their number declined from 62% of total astrocytes in control rats to 41% in rats at 7 days PI. Nestin/ BrdU-positive A2 astrocytes were found only within a distance of ~100 μm from the stab wound and, in comparison to those in control rats, showed an upregulation of K_{DR} currents. Their number increased from 8% of the total number of astrocytes in control rats to 39% 7 days PI. Both A1 and A2 astrocytes showed hypertrophied processes and increased GFAP staining, but an examination of cell morphology revealed greater changes in the surface/volume ratio in A2 astrocytes than in A1 astrocytes. Complex astrocytes did not display a hypertophied morphology; K_{IR} currents in these cells were upregulated within 1 day PI, while the K_{DR}, K_A, and I_{Na} currents were increased only 6 h PI. We conclude that two electrophysiologically, immunohistochemically, and morphologically distinct types of hypertrophied astrocytes are present at the site of a stab wound, depending on the distance from the lesion, and may have different functions in ionic homeostasis and/or regeneration.

Grant number: GACR 305/03/1172; Grant number: GACR 305/02/1528; Grant number: AV0Z5039906; Grant number: MSMT LN00A065; Grant number: MSMT J13/98111300004.

*Correspondence to: Miroslava Anděrová, Department of Neuroscience, Institute of Experimental Medicine, Academy of Sciences of the Czech Republic, Vídeňská 1083, 142 20 Prague 4, Czech Republic.
E-mail: anderova@biomed.cas.cz

Received 13 October 2003; Accepted 14 April 2004

DOI 10.1002/glia.20076

Published online 16 June 2004 in Wiley InterScience (www.interscience.wiley.com).

INTRODUCTION

Central nervous system (CNS) injury and neurodegenerative diseases are often associated with reactive gliosis, characterized by enhanced glial proliferation, astrocytic dedifferentiation, hyperplasia of astrocytes and microglia, and astrocytic hypertrophy, resulting in the formation of a dense astrocytic scar (Norton, 1999). A major hallmark of the astrocytic response to brain injury is the elevated expression of glial fibrillary acidic protein (GFAP) (Bignami and Dahl, 1977; Hozumi et al., 1990).

The membrane properties of post-traumatic astrocytes have been studied in vitro, in cultures of cortical (Bevan et al., 1987; Perillan et al., 1999, 2000) or spinal cord astrocytes (MacFarlane and Sontheimer, 1997, 1998). These studies have demonstrated that proliferating spinal cord astrocytes increased the specific conductance of delayed outwardly rectifying K^+ currents (K_{DR}), transient A-type K^+ currents (K_A), as well as Na^+ currents. Furthermore, a downregulation of inwardly rectifying currents (K_{IR}) was demonstrated in proliferating astrocytes, while nonproliferating astrocytes showed an increase in K_{IR} currents. It has been demonstrated, using different in vivo models of CNS injury, that the changes in voltage-dependent ion channels in post-traumatic astrocytes are affected by the nature and extent of the tissue injury. Westenbroek et al. (1998) described the upregulation of Ca^{2+} channels in response to brain injury, hypomyelination, and ischemia. In contrast, the intracerebroventricular injection of kainate induced the degeneration of hippocampal pyramidal cells in the CA3–C4 region and caused either a loss or reduction of Ca^{2+} channels in astrocytes in acutely isolated hippocampal slices (Burnard et al., 1990). Furthermore, a loss of tetrodoxin-sensitive Na^+ channels in reactive astrocytes in the adult rat hippocampus was reported in a lesion induced by an intraperitoneal injection of kainate (Jabs et al., 1997). In the rat hippocampus, fluid percussion injury induced a reduction in transient K_A and K_{IR} currents (D'Ambrosio et al., 1999). In the dentate gyrus of adult rats that underwent an entorhinal cortex lesion (ECL), a reduction in K_{IR} currents was reported (Schroder et al., 1999). Similar to in vitro models of gliosis (MacFarlane and Sontheimer, 1997, 1998), the expression of voltage-gated K^+ channels in astrocytes in vivo is also affected by astrocyte proliferation at the site of injury. In the cortex of young rats (P16–24) that underwent a focal cortical freeze-lesion on the first postnatal day (P1), bromodeoxyuridine (BrdU)-positive cells showed an enhanced expression of K_{DR} channels, but they did not express K_{IR} channels (Bordey et al., 2000, 2001). Temporal lobe epilepsy (TLE) is also accompanied by reactive gliosis and thus by changes in glial membrane properties (Bordey and Sontheimer, 1998; Hinterkeuser et al., 2000; Schröder et al., 2000). The glial membrane properties either resembled those typical of immature astrocytes, expressing K_{DR}, K_A, K_{IR}, and Na^+ currents, or the cells displayed strong inward rectification.

The astrocytic response to a stab wound is characterized by intense immunostaining for GFAP, (Enclancher et al., 1990; Vijayan et al., 1990; Kálmán and Ajtai, 2000; Nolte et al., 2001), for S-100 , a calcium-binding protein found predominantly in astrocytes, and for vimentin, a cytoskeletal protein that is expressed in reactive astrocytes (Perillan et al., 1999, 2000). Our previous studies have shown that astrogliosis increases diffusion barriers in the CNS due to the hypertrophy of astrocytic processes and the increased production of extracellular matrix components (Syková, 1997; Roitbak and Syková, 1999; Syková and Chvátal, 2000). This can impair the diffusion of ions, neurotransmitters, trophic factors, and other neuroactive substances in the brain and thus influence tissue injury.

In the present study, we have investigated the electrophysiological and immunohistochemical properties of astrocytes around a stab wound in rat cortical slices in situ. In addition, morphology of astrocytes was analyzed using three-dimensional (3D) confocal morphometry. To reveal the functional changes in astrocytes, the changes in the membrane properties of the astrocytes were correlated with the changes in resting extracellular K^+ concentration measured in vivo and with astrocyte proliferation at the site of injury.

MATERIALS AND METHODS

Cortical Stab Wound

Twenty-one-day-old Wistar rats (P21, male, 60–70 g) were anesthetized by an intraperitoneal injection of 60 mg/kg sodium pentobarbital. Core temperature was maintained at 37°C with a heating pad. In the first group of animals, sham-operated rats used as controls, the skull was exposed, and part of the skull was removed with a dental drill. The skin was then sutured. The second group of animals was subjected to a unilateral stab wound (Roitbak and Syková, 1999). Briefly, a fine microdissecting knife was used to make a stab wound in the rostrocaudal direction, 3 mm long and 1.2–1.5 mm deep from the pial surface, 1.5 mm lateral from the midline, and 0.5 mm rostral from the lambda. The skin overlying the cranium was then sutured. At 6 h and 1, 3, 5, and 7 days post-wound, brain slices were prepared and used in patch clamp experiments in situ, or the rats were used for extracellular K^+ measurements in vivo.

Preparation of Acute Brain Slices

The rats were sacrificed under pentobarbital anesthesia (60 mg/kg) at postnatal days 21 to 28 (P21–28) by decapitation. The brain was quickly dissected and placed in artificial cerebrospinal fluid (ACF) at 6–8°C. For patch-clamp recording, the brain was hemisected and glued with tissue adhesive (Electron Microscopy

Science, Hartfield, PA) to a Teflon plate. Transverse 250-μm-thick slices were made using an automatic oscillating tissue slicer EMS-4000 (Electron Microscopy Science). The slices were kept at 22–25°C for up to 6 h in ACF containing (in mM): NaCl 117.0, KCl 3.0, $CaCl_2$ 1.5, $MgCl_2$ 1.3, Na_2HPO_4 1.25, $NaHCO_3$ 35.0, D-glucose 10.0, and osmolality 300 mmol/kg. The solution was continuously gassed with a mixture of 95% O_2 and 5% CO_2 to maintain a final pH value of 7.4. Osmolarity was measured using a vapor pressure osmometer (Vapro 5520; Wescor, Logan, UT).

Patch-Clamp Recordings

Glial membrane currents were recorded with the patch-clamp technique in the whole-cell configuration (Hamill et al., 1981). Recording pipettes with a tip resistance of 4–6 MΩ were made from borosilicate capillaries (Rückl & Sons, Otvovice, Czech Republic) using a Brown-Flaming micropipette puller (P-97; Sutter Instruments, Novato, CA). Electrodes were filled with a solution containing (in mM): KCl 130.0, $CaCl_2$ 0.5, $MgCl_2$ 2.0, EGTA 5.0, Hepes 10.0. The pH was adjusted with KOH to 7.2. The intracellular solution contained 1 mg/ml Lucifer Yellow (LY) Dilithium salt (Sigma, St. Louis, MO) or Alexa Fluor hydrazid 488 (Molecular Probes, Eugene, OR). All recordings were made in slices perfused with ACF at a temperature of 22–25°C.

The cells were approached by the patch electrode, using an INFRAPATCH system (Luigs & Neumann, Ratingen, Germany). The slices were placed in a chamber mounted on the stage of a fluorescence microscope (Axioskop FX, Carl Zeiss, Germany) and fixed using a U-shaped platinum wire with a grid of nylon threads. The cells and the recording electrodes were imaged with an infrared-sensitive video camera (C2400-03; Hamamatsu Photonics, Hamamatsu City, Japan) and displayed on a standard TV/video monitor. Current signals were amplified with an EPC-9 amplifier (HEKA Elektronik, Lambrecht/Pfalz, Germany), lowpass-filtered at 3 kHz and sampled at 5 kHz by an interface connected to an AT-compatible computer system, which also served as a stimulus generator. Data acquisition, storage and analysis were performed with TIDA (HEKA Elektronik, Lambrecht/Pfalz, Germany).

Electrophysiological Measurements and Protocols

Membrane potential (V_m) was measured by switching the EPC-9 amplifier to the current clamp mode. The holding potential was −70 mV. Membrane capacitance (C_m) was determined from the current transients elicited by a 10-mV test pulse depolarizing the cell membrane from −70 to −60 mV.

Current patterns were obtained by clamping the cell membrane from the holding potential of −70 mV to values ranging from −160 mV to +20 mV at intervals of 10 mV. Pulse duration was 50 ms. To isolate voltage-gated K_{DR} and K_{IR} current components, the voltage step from −70 to −60 mV was used to subtract the time- and voltage-independent currents (Chvátal et al., 1995; Pastor et al., 1995). Briefly, the small time- and voltage-independent current recorded at −60 mV was multiplied by the relative potential jumps and then subtracted from the measured current. The amplitudes of delayed outwardly rectifying K^+ currents (K_{DR}) were measured at +20 mV, at the end of the pulse. The A-type K^+ current (K_A) component was isolated by subtracting the current traces clamped at −110 mV from those clamped at −70 mV, and its amplitude was measured at +20 mV at the peak value. The amplitudes of inwardly rectifying K^+ currents (K_{IR}) were measured at −160 mV at the end of the pulse. TTX-sensitive Na^+-currents were isolated by subtracting the current traces measured in 5–10μM TTX-containing solution from those measured under control conditions. Na^+ current amplitudes were measured at the peak value.

In Vivo Measurements of Resting Extracellular K^+ Concentration

The rats were anesthetized with sodium pentobarbital (60 mg/kg) and placed in a rat head holder. The rats breathed spontaneously. Body temperature was maintained with a heating pad at 37 °C. A part of the skull was removed with a dental drill to reach the wounded part of the cortex. During experiments, the exposed cortex was continuously superfused with ACF (37 °C). The resting extracellular K^+ concentration was measured by means of double-barreled K^+-sensitive microelectrodes (K^+-ISMs) as described elsewhere (Syková et al., 1994). The liquid ion-exchanger sensitive to K^+ was Corning 477317. The K^+-sensitive barrel of the microelectrode was back filled with 0.5 M KCl, while the reference barrel contained 150 mM NaCl. K^+-ISMs were calibrated in solutions containing 2, 3, 4, 6, 12 and 20 mM KCl in 150 mM NaCl. To keep the solutions iso-osmolar (300 mmol/kg), ACF containing 4 − 20 mM K^+ had a reciprocally reduced Na^+ concentration. Using a micromanipulator, the microelectrode was lowered into the cortex to depths of 500, 1,000, and 1,500 μm from the cortical surface in the middle of the stab wound and also at distances of 500 and 1,000 μm from the stab wound.

Immunohistochemistry

To visualize recorded cells in the slices, the cells were filled with LY by dialyzing the cytoplasm with the patch pipette solution. The slices were fixed with 4% paraformaldehyde in 0.1 M phosphate buffer (PB; pH 7.5) overnight at 5°C and then washed and kept in 0.1 M PB at 5°C.

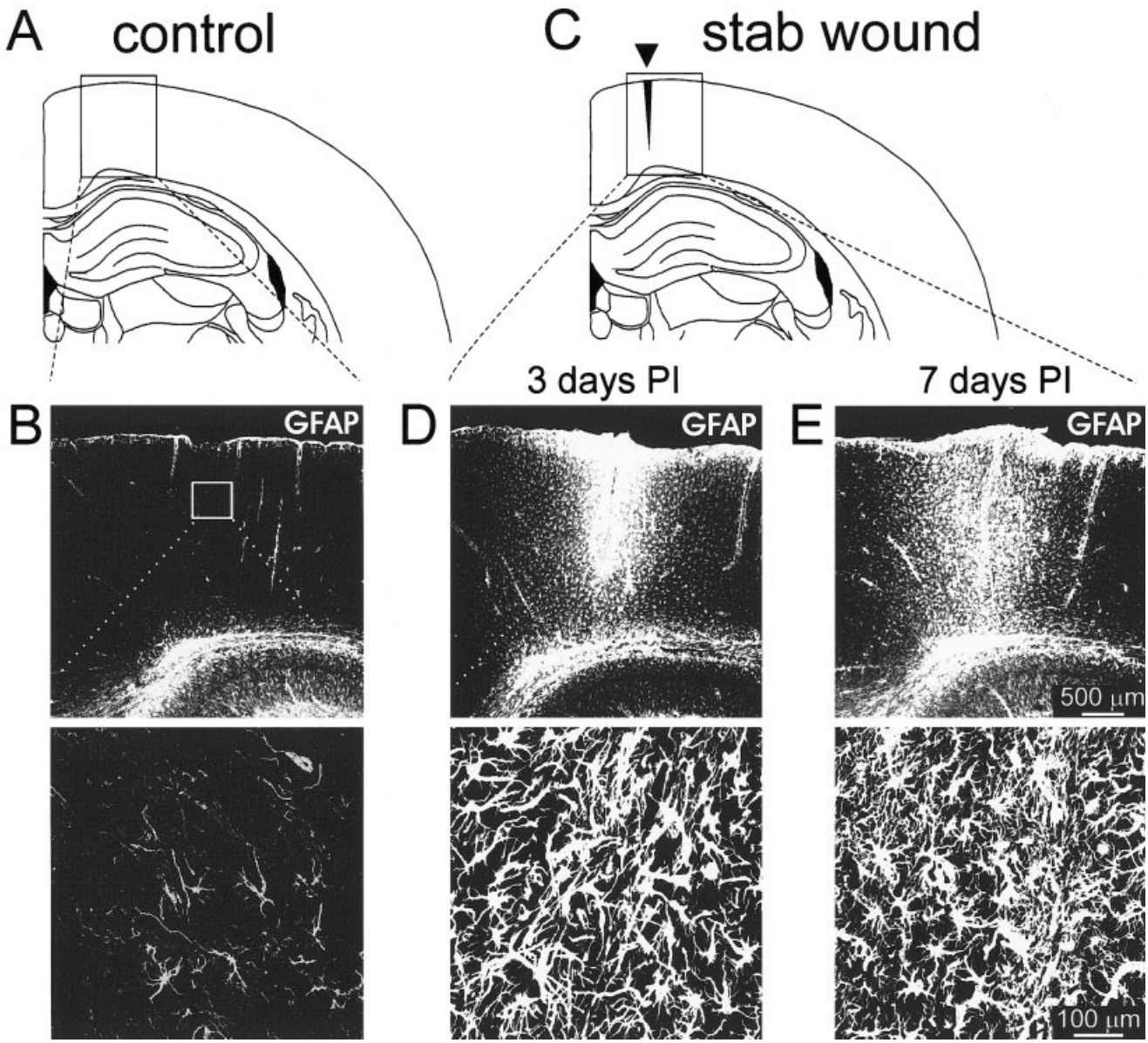

Fig. 1. Reactive gliosis in the rat cortex, immunostained for glial fibrillary acidic protein (GFAP) after a cortical stab wound. Immunohistochemistry of coronal sections from control cortex (**A,B**), and from the cortex of injured rats 3 days (**C,D**) and 7 days (**C,E**) post-injury (PI). Sections of the brain slices indicated in A and C were stained for GFAP. Upper photomicrographs (**B–E**) show the cortex in control and wounded animals, the lower photomicrographs show a higher magnification of the areas highlighted by squares in the upper panels. Note the stronger expression of GFAP in the vicinity of the stab wound.

To identify the recorded cells as astrocytes, an antibody directed against GFAP was used. Slices were incubated overnight at 4°C with a mouse monoclonal antibody directed against GFAP and conjugated with Cy3 (Sigma), diluted 1:200 in phosphate-buffered saline (PBS) containing 1% bovine serum albumin (BSA; Sigma) and 0.5% Triton X-100 (Sigma). To identify cells as astrocytes or their precursors, slices were incubated overnight at 4°C with a mouse monoclonal antibody directed against the subunit S-100β protein (Sigma), diluted 1:200 in PBS containing 1% BSA and 0.5% Triton X-100, followed by incubation with the secondary antibody, goat anti-mouse IgG conjugated with Alexa 594 (Molecular Probes). After immunostaining the slices were mounted using Vectashield mounting medium (Vector Laboratories, Burlingame, CA).

To identify proliferating astrocytes, antibodies directed against BrdU (Roche Diagnostics GmbH, Mannheim, Germany) and GFAP were used. To identify newly generated astrocytes or reactive astrocytes, antibodies directed against nestin (Chemicon, Temecula, CA) and GFAP were employed. Antibodies against BrdU and doublecortin (DCX-18; Santa Cruz Laboratories, Santa Cruz, CA) were used to identify newly generated neurons in the brain in response to injury. Four intraperitoneal injections of BrdU (75 mg/kg),

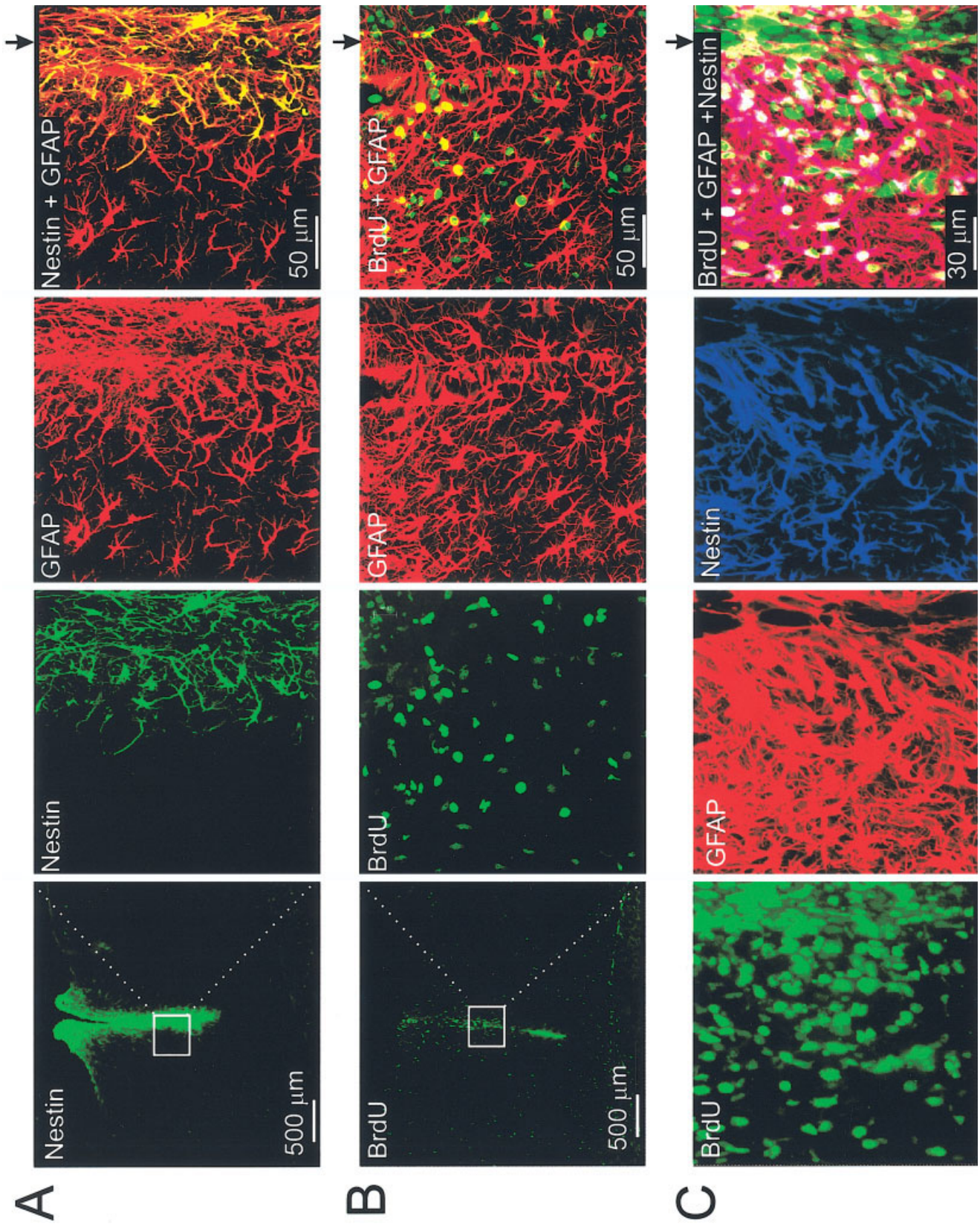

Fig. 2. Reactive gliosis in the rat cortex, immunostained for glial fibrillary acidic protein (GFAP), nestin, and BrdU after a cortical stab wound. **A:** Immunostaining for nestin (left; low magnification) and double immunostaining for nestin and GFAP (right; high magnification) in the cortex of a wounded rat 3 days post-injury (PI). Note the presence of nestin-positive astrocytes (nestin+GFAP) only in the vicinity of the wound; double stained cells are yellow. **B:** Immunostaining for BrdU (left; low magnification) and double immunostaining for BrdU and GFAP (right; high magnification) in the cortex of a wounded rat 3 days PI. Note the increased proliferation of astrocytes (BrdU+GFAP) only in the vicinity of the stab wound; double stained cells are yellow. **C:** Triple immunostaining for BrdU, GFAP, and nestin in the cortex of a wounded rat at 3 days PI. Double-stained cells are violet; triple stained cells are white. Arrowheads in A–C indicate the site of the stab wound.

TABLE 1. Membrane Properties of A1, A2, and Complex Astrocytes in Control and Injured Rat Cortex, 3 and 7 days After Stab Wound†

		Control	3 days PI	7 days PI
A1 astrocytes				
V_m	[mV]	−75.77 ± 1.05	−69.91 ± 1.92**	−72.82 ± 1.28
C_m	[pF]	84.16 ± 18.54	92.73 ± 20.12	83.10 ± 19.41
IR	[MΩ]	70.10 ± 5.94	61.40 ± 12.00	97.95 ± 11.41
K_{IR}/C_m	[pA/pF]	1.23 ± 0.36	3.82 ± 1.60***	2.32 ± 0.94
n		49	24	45
A2 astrocytes				
V_m	[mV]	−76.25 ± 2.01	−72.55 ± 2.21	−70.52 ± 1.68
C_m	[pF]	50.60 ± 13.50	49.19 ± 6.62	58.38 ± 9.65
IR	[MΩ]	57.32 ± 7.04	153.84 ± 41.93	151.66 ± 24.90*
K_{DR}/C_m	[pA/pF]	2.22 ± 0.50	11.67 ± 2.43*	22.83 ± 3.40*
n		6	17	47
Complex astrocytes				
V_m	[mV]	−84.02 ± 1.56	−78.10 ± 5.20	−79.65 ± 1.78
C_m	[pF]	24.94 ± 5.93	26.20 ± 3.41	22.15 ± 6.06
IR	[MΩ]	195.91 ± 18.36	284.21 ± 42.85*	315.95 ± 41.63**
K_{DR}/C_m	[pA/pF]	27.55 ± 4.40	35.18 ± 4.99	34.72 ± 18.80
K_A/C_m	[pA/pF]	28.15 ± 9.30	32.88 ± 5.45	37.72 ± 7.28
K_{IR}/C_m	[pA/pF]	8.11 ± 1.49	9.11 ± 2.68	3.55 ± 1.15*
I_{Na}/C_m	[pA/pF]	10.76 ± 2.26	10.88 ± 4.42	15.72 ± 2.55
n		25	8	23

V_m, membrane potential; C_m, membrane capacitance; IR, input resistance; K_{DR}/C_m, K_A/C_m, K_{IR}/C_m, I_{Na}/C_m, K_{DR}, K_A, K_{IR}, I_{Na}, current densities; n, number of cells.
†Statistical significance was evaluated as the difference between control and wounded rats (***$P < 0.001$,**$P < 0.01$, *$P < 0.05$ unpaired, two-tailed t-test).

spaced 6 h apart, were given to control rats (n = 2) and wounded rats 1, 3, 5, or 7 days after surgery (n = 8). After 24 h, the animals were anesthetized (100 mg/kg sodium pentobarbital) and perfused transcardially with 100 ml of 0.9% saline, followed by 200 ml of 4% paraformaldehyde (in 0.1 M PB, pH 7.4). Brains were dissected out and postfixed in paraformaldehyde solution overnight and then placed in 30% sucrose in 0.1 M PB and allowed to sink (24–36 h) for cryoprotection. Coronal slices, 80μm thick, were prepared using a microtome. Free-floating sections were incubated with mouse monoclonal anti-BrdU followed by mouse monoclonal anti-nestin and goat anti-DCX (all diluted 1:100 in PBS containing 1% BSA) to identify newly generated neurons. To detect newly generated astrocytes, mouse monoclonal anti-GFAP conjugated with Cy3 was substituted for anti-DCX in the second incubation. BrdU-positive, nestin-positive and DCX-positive cells were visualized using the appropriate secondary antibody, either goat anti-mouse IgG or donkey anti-goat IgG, conjugated with Alexa 488, 594, or 633 (Molecular Probes). After immunostaining, the slices were examined using a LEICA TCS SP system spectral confocal microscope equipped with an Arg/HeNe laser.

Confocal Morphometry

Changes in cell morphology were quantified by analyzing the cell surface/volume ratio from images of Lucifer yellow-filled glial cells obtained by a LEICA TCS SP system confocal microscope equipped with an Arg/HeNe laser. The image of a cell was sectioned into a uniformly spaced (0.12-μm) set of two-dimensional (2D) parallel images. The cell surface was found in each image using an edge-detecting algorithm, and the area of the image surrounded by the edge was calculated for each image. The values of cell surface and volume for individual cells were obtained by integrating the values of the edge length and area from all images in a set.

Statistical Analysis

The results are expressed as the mean ± SEM. Statistical analysis of the differences between groups was evaluated using a t-test. Values of $P < 0.05$ were considered significant.

RESULTS

Immunohistochemistry of the Stab Wound

Astrocytic changes were investigated immunohistochemically in a total of 13 animals, prior to and 1, 3, 5, and 7 days post-injury (PI). Compared with control rats, the immunohistochemical analysis of brain slices from wounded animals (P21–28) showed increased GFAP immunoreactivity at the site of injury from 1 to 7 days PI (Fig. 1), an immunohistochemical pattern similar to that described previously (Hozumi et al., 1990; Roitbak and Syková, 1999). Typical hypertrophied astrocytes, with thickened processes and enlarged cell bodies, were found in the area surrounding the stab wound, while no changes in GFAP immunoreactivity were observed in the contralateral hemisphere. In addition to GFAP, nestin, an intermediate filament abundantly expressed in the developing CNS, was used

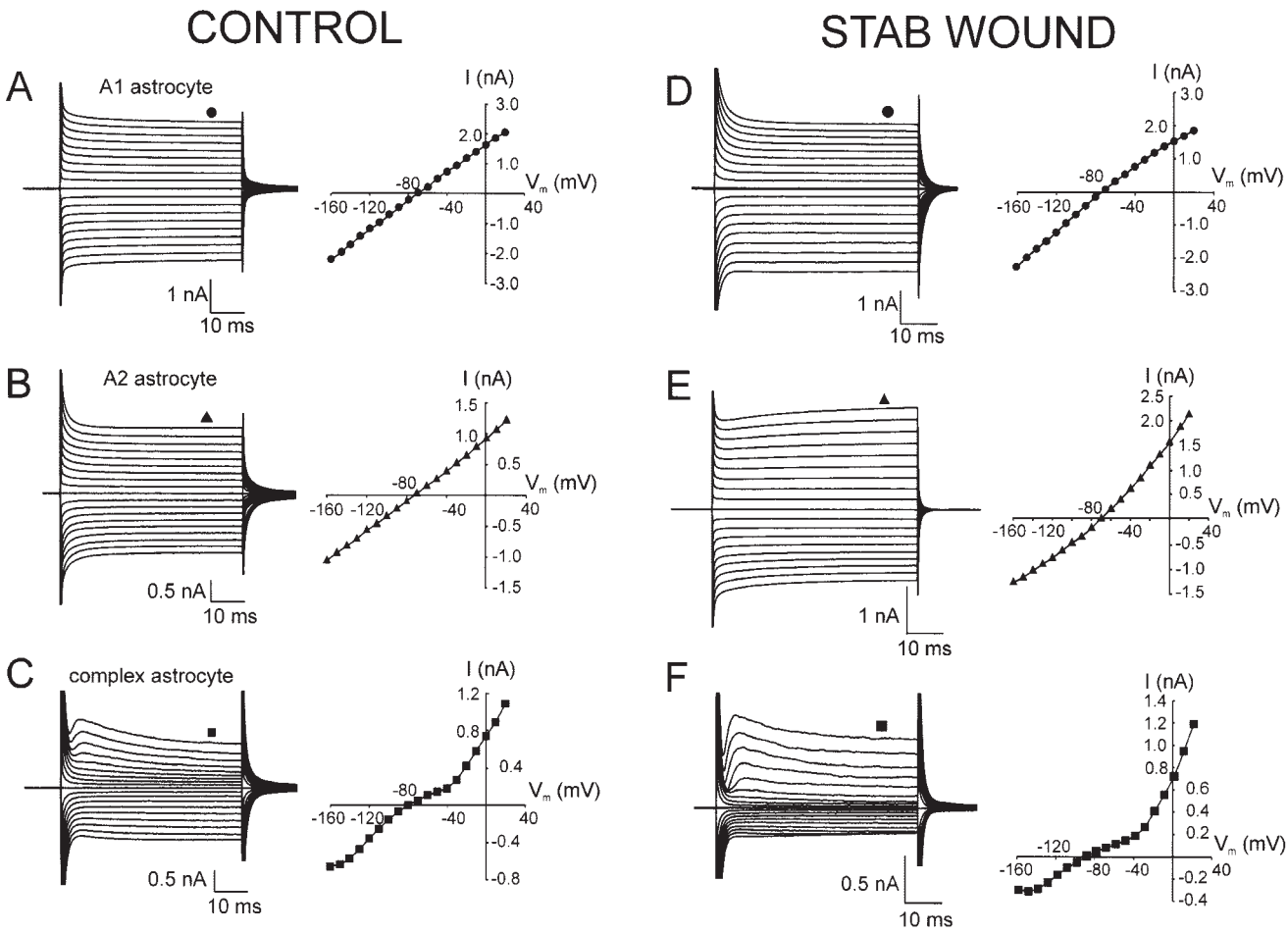

Fig. 3. Typical membrane current patterns of astrocytes in the cortex of control rats and 7 days post-injury (PI). Membrane current patterns and the current/voltage relationship in A1 astrocytes (**A,D**), A2 astrocytes (**B,E**) and complex astrocytes (**C,F**) were measured in response to voltage steps from a holding potential of −70 mV. To activate the currents, the membrane was clamped for 50 ms from the holding potential of −70 mV to increasing de- and hyperpolarizing potentials ranging from −160 to +20 mV, in 10-mV increments.

as an earlier and more sensitive marker of astrocyte activation (Frisen et al., 1995). Increased nestin immunoreactivity was observed from 1 to 7 days PI, in the vicinity of the stab wound (Fig. 2A, left) and in the dentate gyrus. Double-stained, nestin/GFAP-positive cells were observed only within a distance of ~100 μm from the stab wound (Fig. 2A, right), while nestin/DCX-positive cells were observed only in the dentate gyrus (not shown).

Increased cell proliferation was found at the site of the stab wound. BrdU, a DNA marker that is selectively incorporated by dividing cells during the S-phase of the cell cycle, was used to identify proliferating cells. In control animals, only a few BrdU-positive cells were found in brain sections, while in wounded animals increased BrdU staining was observed in the ipsilateral as well as the contralateral hemisphere. The largest number of BrdU-positive cells was seen 3 days PI in the vicinity of the stab wound (Fig. 2B, left), but also in the corpus callosum, dentate gyrus, and in a region at the side of the lateral ventricle (fimbria) of both the ipsilateral and contralateral hemispheres. GFAP/BrdU-positive cells were found only close to the wound (Fig. 2B, right). No increased BrdU staining was seen in the cortex of the contralateral hemisphere. Five days PI, BrdU immunoreactivity declined, and at 7 days PI only a very few cells were BrdU-positive. Triple-stained, nestin/BrdU/GFAP-positive cells were found only in the vicinity of the stab wound (Fig. 2C, right).

We conclude that there are two immunohistochemically distinct types of astrocytes around the stab wound: GFAP/nestin/BrdU-positive astrocytes and GFAP-positive astrocytes only.

Membrane Properties and Morphology of Astrocytes in the Gliotic Cortex

The changes in the membrane properties of astrocytes around a cortical stab wound were studied using the patch-clamp method in the whole-cell configuration in acute cortical slices at 6 h and 1, 3, 5, and 7 days PI, in 338 cells from 103 rats. The rats were 21–28 days

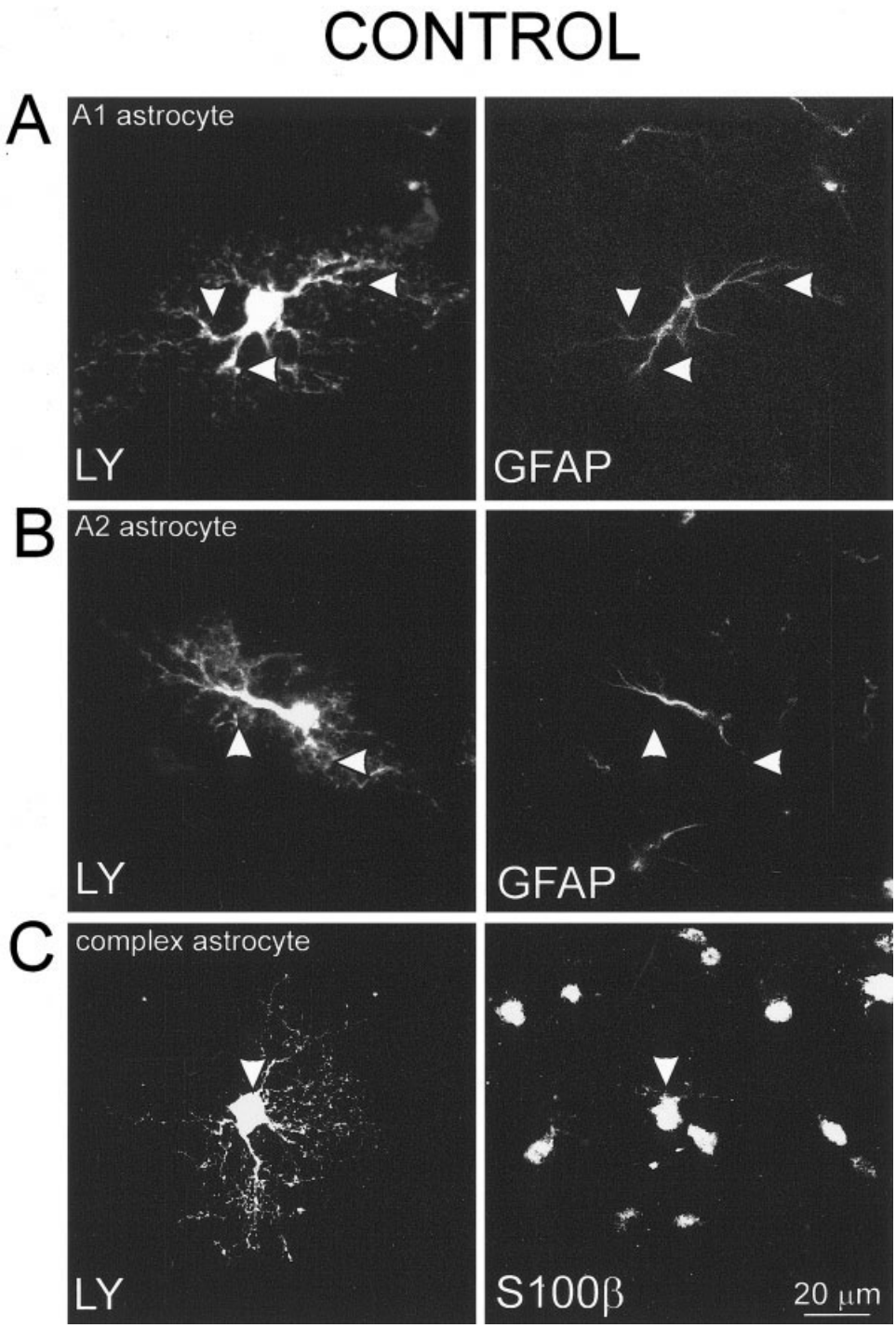

Fig. 4. Typical morphology and immunohistochemical identification of astrocytes in the cortex of control rats and 7 days post-injury (PI). During the electrophysiological recordings shown in Fig. 3, A1 astrocytes (**A,D**), A2 astrocytes (**B,E**), and complex astrocytes (**C,F**) were filled with Lucifer Yellow and subsequently examined under a confocal microscope. Lucifer Yellow-filled A1 astrocytes and A2 astrocytes were identified by positive staining for glial fibrillary acidic protein (GFAP), while most complex astrocytes were positive for S-100β. Arrowheads indicate similar patterns in both images.

old. The recorded cells were electrophysiologically identified as astrocytes by the lack of an action potential during seal formation and during current clamp recording. Following patch-clamp recordings, 114 cells (46%) out of 247 immunostained cells expressing a typical astrocytic current pattern were either GFAP- or S-100β-positive. The following membrane parameters were compared: membrane potential (V_m), input resistance (IR), membrane capacitance (C_m), and K_{DR}, K_A, K_{IR}, and I_{Na} current densities (Table 1).

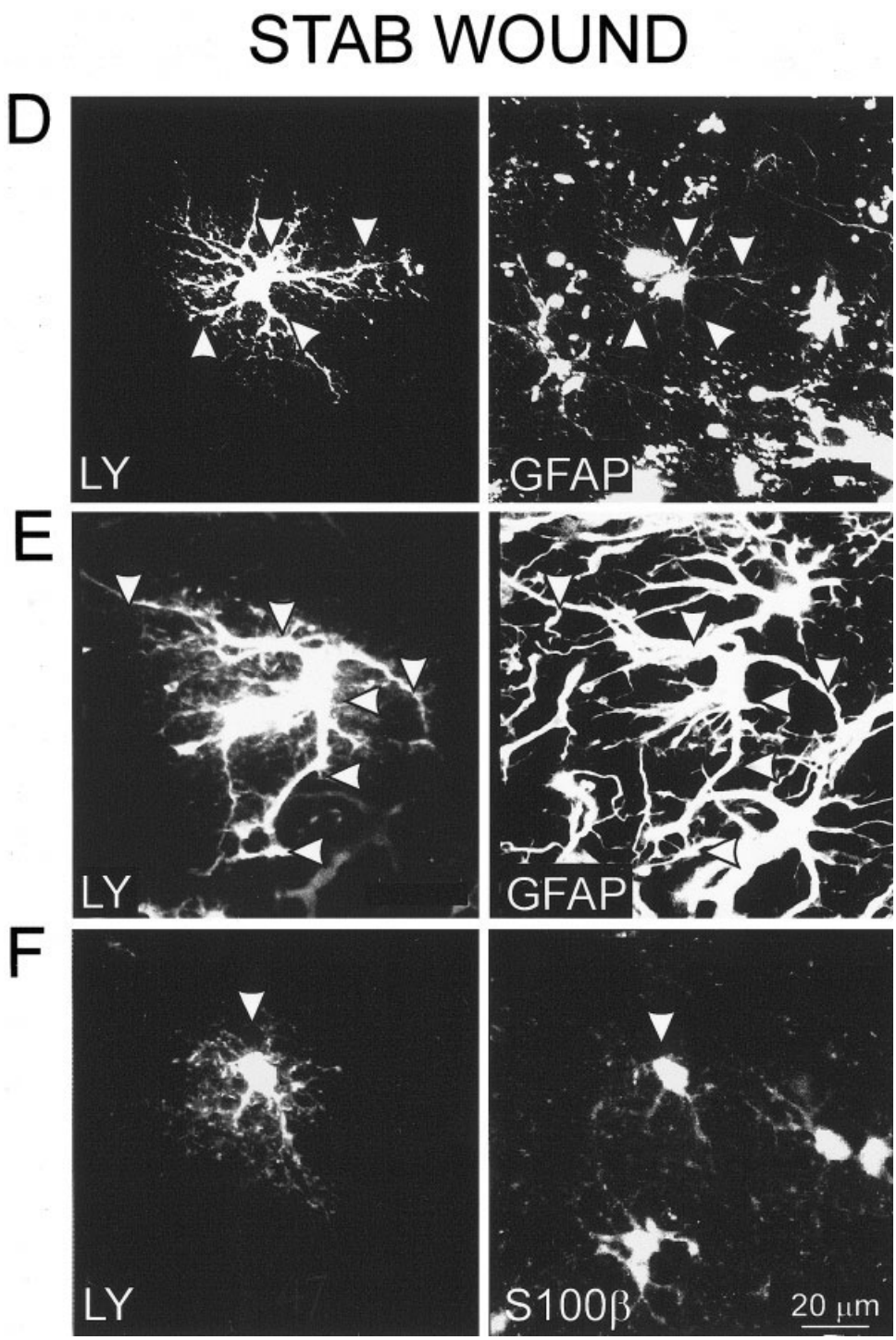

Figure 4. (Continued)

Three electrophysiologically and morphologically distinct types of astrocytes were found in the cortex of control rats (Fig 3 and Fig 4). Forty-nine astrocytes (61%) had a large time- and voltage-independent K^+ current component, but they also displayed inwardly rectifying K^+ currents that became most apparent following leak subtraction (A1 astrocytes, Fig. 3A). Six astrocytes (8%) displayed a large time- and voltage-independent K^+ current component with the additional expression of outwardly rectifying K^+ currents that were apparent following leak subtraction (A2 astrocytes, Fig. 3B). Twenty-five astrocytes (31%) expressed a combination of time- and voltage-activated currents that include A-type (K_A), delayed outwardly rectifying (K_{DR}) and inwardly rectifying K^+ currents (K_{IR}), as well as Na^+ channels (I_{Na}, Fig.

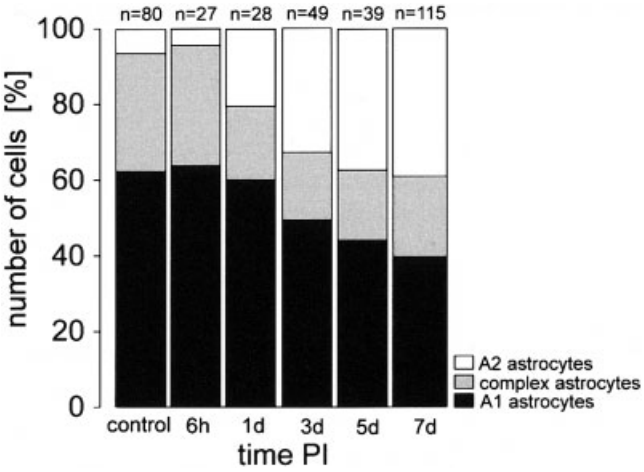

Fig. 5. Changes in the ratio of A1, A2, and complex astrocytes evoked by a cortical stab wound. The total number (100%) of cells was calculated by summing all measured A1, A2, and complex astrocytes at each time point, before (control) and 6 h and 1, 3, 5, and 7 days after stab wound. The numbers of A2 (white columns), A1 (black columns) and complex astrocytes (gray columns) are represented in the graph. Note the increasing number of A2 astrocytes and the declining number of A1 and complex astrocytes.

3C). These cells were previously termed complex astrocytes. We found no differences between the membrane properties of A1 and A2 astrocytes, except for the differential expression of K_{IR} and K_{DR} currents in A1 and A2 astrocytes, respectively (Table 1). Complex astrocytes differed from both A1 and A2 astrocytes by a more negative V_m, higher IR values, and lower C_m (Table 1).

Similar to the case in control animals, we found three types of astrocytes around the stab wound. A1 astrocytes (n = 45, Fig. 3D) were found at distances greater than ~100 μm from the wound, while A2 astrocytes (n = 47, Fig. 3E) were found only within a distance of ~100 μm from the wound. Three days PI, A1 astrocytes differed from those in control rats by their decreased V_m, while 7 days PI their membrane properties were similar to controls (Table 1). Their number declined from 61% of the total number of astrocytes in controls to 41% 7 days PI (Fig. 5). In A2 astrocytes, we found an increase in IR and K_{DR} current density 3 and 7 days PI (Table 1). The number of A2 astrocytes was 8% in control rats, while 3 days PI the percentage was significantly higher and reached 39% at 7 days PI (Fig. 5). Complex astrocytes (n = 23, Fig. 3F) showed increased IR 3 and 7 days PI and a decrease in K_{IR} current density 7 days PI. Their number declined from 31% to 20% 7 days PI.

Quantification of the morphological changes in astrocytes induced by a cortical stab wound was performed in 23 cells from 11 animals by 3D reconstruction of LY-labeled astrocytes, using confocal microscopy. We did not find any significant differences in the morphology of complex astrocytes between control and wounded rats (see Fig. 4C,F); therefore, cell morphometry was performed only on A1 and A2 astrocytes. The morphology of astrocytes from control and wounded animals was characterized by the cell surface-to-cell volume ratio (S/V). In control rats, the morphology of A1 astrocytes was not significantly different from that of A2 astrocytes, and the mean S/V for both was 5.37 ± 0.62 (n = 5). In contrast, the morphology of A1 and A2 astrocytes differed 7 days PI. The A2 astrocytes displayed typical features of reactive astrocytes, i.e., hypertrophy, increased GFAP staining and end-feet-like structures at the end of some processes (Fig. 4E), while A1 astrocytes retained almost the same appearance as control A1 astrocytes (Fig. 4A,D). There was no hypertrophy or increased GFAP staining in these cells as in A2 astrocytes. In comparison to A2 and A1 astrocytes in control rats, at 7 days PI both types of astrocytes showed a decrease in their S/V ratio, reflecting changes in cell volume. The mean S/V was 3.54 ± 0.42 (n = 7) in A1 astrocytes and 2.5 ± 0.19 (n = 11) in A2 astrocytes. We conclude that 7 days PI, A2 astrocytes had a significantly increased cell volume compared with control, as well as to A1, astrocytes.

Changes in K_{IR} Currents in A1 and Complex Astrocytes Evoked by a Stab Wound and Their Correlation With Resting Extracellular K^+ Concentration

A1 astrocytes, as well as complex astrocytes, expressed K_{IR} currents with fast activation and without inactivation at the most negative potentials (from −130 to −160 mV). The K_{IR} currents were almost completely blocked after exposure to 1 mM $CsCl_2$, a selective blocker of K_{IR} (Fig. 6A–D). At 7 days PI, we found a significant reduction in K_{IR} current amplitude in complex astrocytes in comparison to those in control rats, while no changes in A1 astrocytes were observed (Table 1). It has already been shown, in post-traumatic astrocytes in in situ preparations, that K_{IR} currents are downregulated (D'Ambrosio et al., 1999; Schroder et al., 1999) or upregulated (Bordey et al., 2000). The changes in K_{IR} current amplitude can be affected by the type of injury; however, they also might be time-dependent and related to $[K^+]_e$, which is significantly increased following injury. Therefore, we studied the changes in K_{IR} current densities at 6 h and 1, 3, 5, and 7 days PI, in 22 rats, and correlated these changes with resting extracellular K^+ concentration ($[K^+]_e$) measured in vivo at the same time intervals, using K^+ ion-sensitive microelectrodes (K^+-ISMs). Changes in $[K^+]_e$ around the stab wound were measured at a depth of 0.5–1.0 mm from the cortical surface and at a distance of 0.5–1.0 mm from the stab wound.

In control rats, the average K_{IR} current densities of complex and A1 astrocytes were 8.11 ± 1.49 pA/pF (n = 25) and 1.23 ± 0.36 pA/pF (n = 49), respectively. $[K^+]_e$ in the cortex of control animals was 3.1 ± 0.1 mM (n =

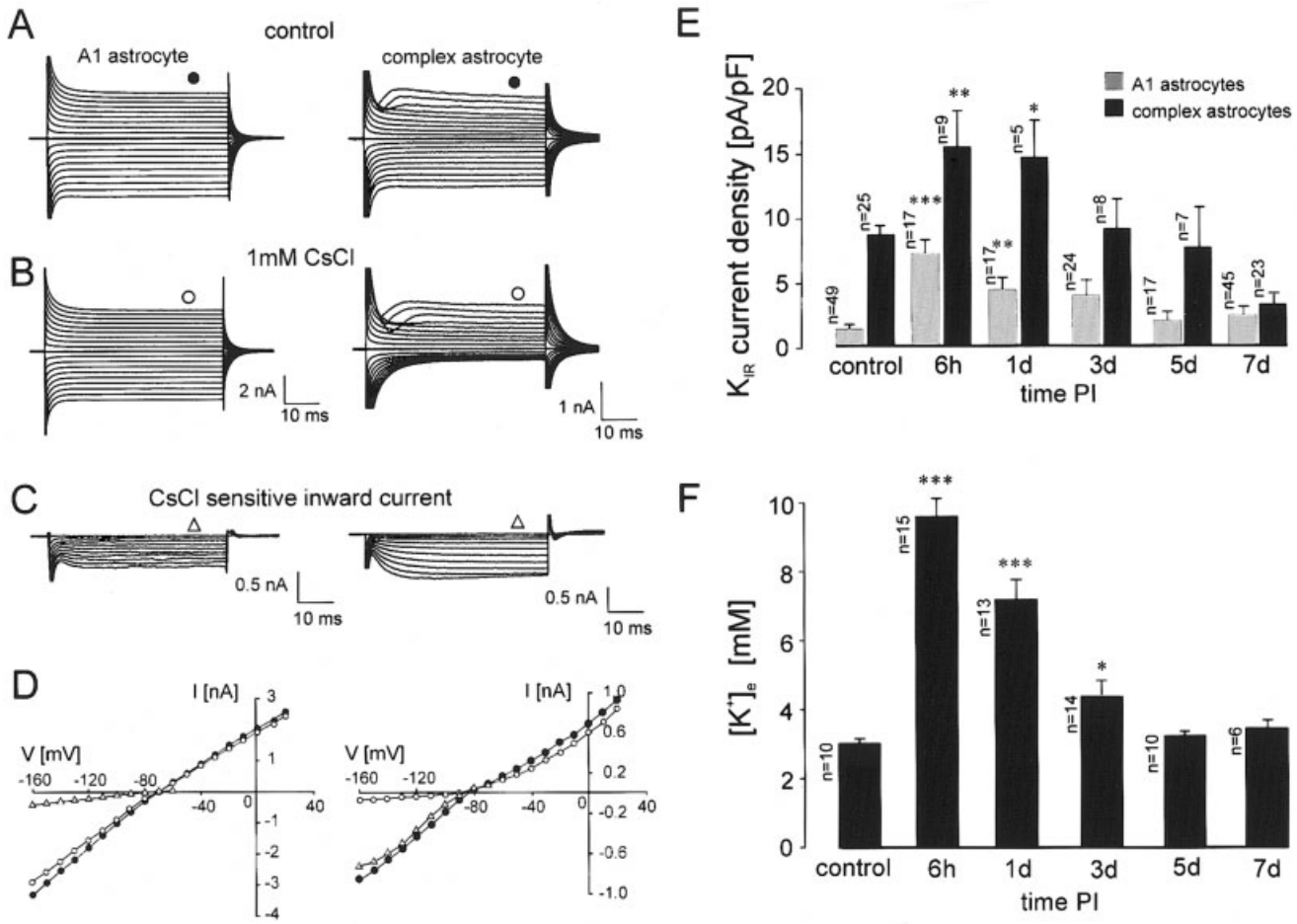

Fig. 6. Cs^+-sensitive voltage-dependent inward currents in A1 and complex astrocytes and extracellular K^+ concentration during the first 7 days after a stab wound. Membrane currents were recorded in response to voltage steps as described in the legend to Figure 3. The membrane current patterns are shown in A1 (**A**, left) and complex (**A**, right) astrocytes prior to the application of 1 mM CsCl (**A**, control), and in the presence of 1 mM CsCl (**B**). **C:** Currents sensitive to CsCl, obtained by subtracting the current traces in the presence of CsCl from the control current traces. The current/voltage (I-V) relationships are shown for the control current traces of A1 (**D**, left) and complex astrocytes (**D**, right) (filled circles), the current traces in the presence of CsCl (empty circles) and Cs^+-sensitive K^+ inward currents (empty triangles). The I-V plot reveals that the inward K^+ currents in A1 and complex astrocytes are Cs^+-sensitive. **E:** Changes in K_{IR} current amplitude at 6 h and 1, 3, 5, and 7 days post-injury (PI), expressed as K_{IR} current density; these currents were correlated with resting extracellular K^+ concentration measured by K^+-selective microelectrodes in the vicinity of the stab wound in vivo (**F**). Note that the time course of changes in K_{IR} current densities and extracellular K^+ is similar. Stars indicate a significant increase when compared with control. ($^*P < 0.05$, $^{**}P < 0.001$, $^{***}P < 0.0001$).

10). At 6 h PI, $[K^+]_e$ reached a value of 9.3 ± 0.5 mM (n = 15), and K_{IR} current densities were significantly increased in both complex and A1 astrocytes (Fig. 6E,F). Within 1–3 days PI, $[K^+]_e$ declined from 7.3 ± 0.4 mM (n = 13) to 4.4 ± 0.4 mM (n = 14), as did K_{IR} current densities in both types of astrocytes. At 5 and 7 days PI, $[K^+]_e$ and K_{IR} current densities in A1 and complex astrocytes returned to their control values. In complex astrocytes, K_{IR} current density was even reduced.

We conclude that K_{IR} currents, which are known to be involved in extracellular K^+ buffering (Verkhratsky and Steinhäuser, 2000), are upregulated in complex and A1 astrocytes within the first day PI, and this upregulation correlates with an increase in resting $[K^+]_e$ in the wounded area of the cortex.

Changes in Delayed Outwardly Rectifying K^+ Currents in A2 Astrocytes Evoked by a Stab Wound

Analysis of A2 astrocytes in the vicinity of the stab wound revealed that they are characterized by hypertrophied processes, enlarged cell bodies and the increased expression of GFAP, and they displayed sustained outward K^+ currents in addition to passive conductance. The outward K^+ currents were elicited by potentials more positive than −60 mV, and they did not inactivate during the voltage step. To identify these currents, we applied 2 mM 4-aminopyridine (4-AP), a known blocker of K_{DR} channels (Fig. 7A–C) and subsequently 10 mM TEA together with 2 mM 4-AP (not shown). We found that ~63% of the K_{DR} currents were

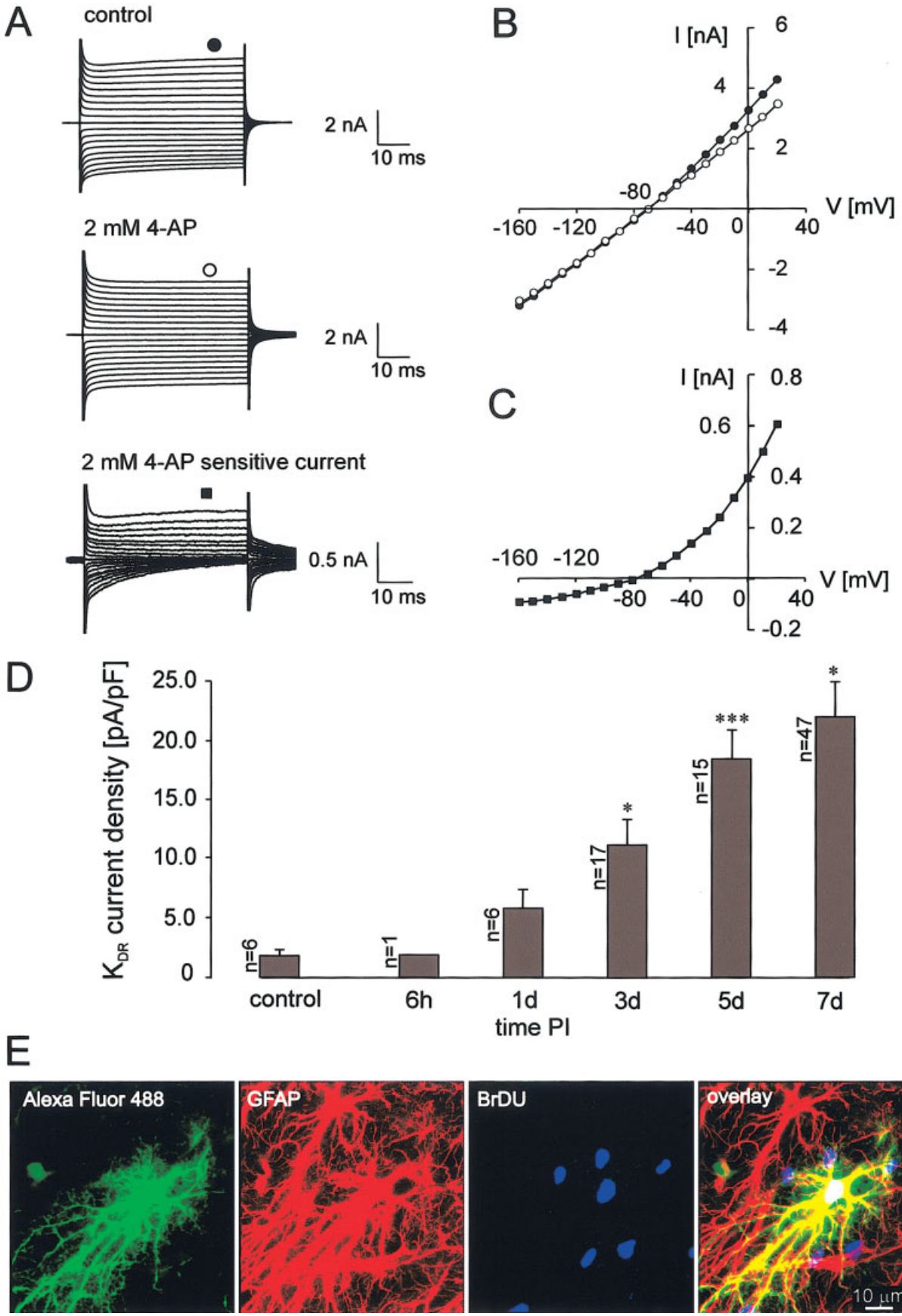
A
control
2 nA
10 ms
2 mM 4-AP
2 nA
10 ms
2 mM 4-AP sensitive current
0.5 nA
10 ms
B
I [nA]
6
4
2
-80
V [mV]
-160 -120 -40 0 40
-2
-4
C
I [nA]
0.8
0.6
0.4
0.2
-160 -120
-80 -40 0 40
V [mV]
-0.2
D
K_DR current density [pA/pF]
25.0
20.0
15.0
10.0
5.0
0
n=6
n=1
n=6
n=17
n=15
n=47
*
***
*
control
6h
1d
3d
5d
7d
time PI
E
Alexa Fluor 488
GFAP
BrDU
overlay
10 µm

Fig. 7.

sensitive to 2 mM 4-AP and ~17% of the K_{DR} currents were blocked by 10 mM TEA. Thus, K_{DR} currents in these astrocytes contain two components, 4-AP- and TEA-sensitive. The residual outward K^+ currents (about 20%) were blocked, together with passive currents, by 10 mM $BaCl_2$, showing that the passive and K_{DR} currents are mainly carried by K^+ (not shown).

To determine how these K_{DR} currents develop after a stab wound, we examined A2 astrocytes 6 h and 1, 3, 5, and 7 days PI. In control rats, the average K_{DR} current density was 2.2 ± 0.5 pA/pF (n = 6) and increased up to 22.8 ± 3.4 pA/pF 7 days PI (n = 47, Fig. 7D).

Triple immunohistochemistry for nestin, BrdU, and GFAP demonstrated that a large number of proliferating cells in the close vicinity of the stab wound were astrocytes (Fig. 2C, right). To confirm that the increased appearance of astrocytes displaying K_{DR} currents around the stab wound correlates with astrocyte proliferation, we used BrdU-injected rats for the electrophysiological identification of A2 astrocytes combined with double BrdU and GFAP immunohistochemistry. Of 8 cells stained post-recording, 2 cells were BrdU/GFAP positive (Fig. 7E). These cells expressed K_{DR} currents in addition to passive conductance and showed hypertrophied processes, an enlarged cell body, increased expression of GFAP, as well as positive BrdU staining.

We conclude that after a cortical stab wound, the upregulation of K_{DR} currents in A2 astrocytes is linked to the increased proliferation of astrocytes at the wound site.

Changes in Outwardly Rectifying K^+ Currents and Na^+ Currents in Complex Astrocytes Evoked by a Stab Wound

In complex astrocytes, we did not find any differences in the current densities of K_{DR}, K_A or Na^+ channels 3 and 7 days PI (Table 1); however, they were significantly increased 6 h PI. In control rats, the K_{DR} and K_A current densities in complex astrocytes were 27.6 ± 4.4 pA/pF and 28.2 ± 9.3 pA/pF (n = 25), respectively, and Na^+ current density was 10.8 ± 2.3 pA/pF. At 6 h PI, the Na^+ current density increased to 23.2 ± 8.1 pA/pF (n = 9, $P = 0.02$), K_A current density to 65.2 ± 11.8 pA/pF ($P = 0.001$) and K_{DR} current density to 49.9 ± 13.9 pA/pF ($P = 0.03$). From the first day PI, the K_A, K_{DR} and Na^+ current densities in complex astrocytes were similar to those in control rats.

Fig. 7. A2 astrocytes display 4-aminopyridine-sensitive outward K^+currents and are BrdU-positive. Membrane currents were recorded in response to voltage steps as described in the legend to Fig. 3. **A:** The membrane current pattern in A2 astrocytes is shown prior to the application of inhibitors (control, top) and in the presence of 2 mM 4-AP (middle). The 2 mM 4-AP-sensitive current was obtained by subtracting the currents after 4-AP application from control currents (bottom). **B:** The resulting current/voltage (I-V) relationships for the control traces (filled circles) and the traces in the presence of 4-AP (empty circles). **C:** The I-V relationship of the 4-AP-sensitive outward K^+ current (filled squares). The I-V plot reveals that the outward K^+ currents in astrocytes found in the vicinity of a stab wound are mainly 4-AP-sensitive. **D:** The changes in outward K^+ currents were analyzed before and then 6 h, 1, 3, 5, and 7 days post-injury (PI). Note that the density of K_{DR} currents increased with time, reaching a maximum 7 days PI. Stars indicate a significant increase, compared with control. (*$P < 0.05$, **$P < 0.001$, ***$P < 0.0001$). **E:** Typical immunostaining of an astrocyte expressing delayed outwardly rectifying K^+currents. The astrocyte was labeled during patch-clamp recording with Alexa Fluor hydrazide 488 and is GFAP- and BrdU-positive.

DISCUSSION

In the present study, we have shown the presence of two types of hypertrophied astrocytes in the gliotic cortex based on their electrophysiological, morphological, and immunohistochemical properties: proliferative astrocytes that appear only in the vicinity of the stab wound and that express delayed outwardly rectifying K^+ currents (A2 astrocytes); and astrocytes that express inwardly rectifying K^+ currents (A1 astrocytes) and are never found close to the stab wound. We have also demonstrated differences in the cell surface/volume ratio between A1 and A2 astrocytes and shown changes in the densities of voltage-dependent K^+ currents, correlated with astrocyte proliferation and the elevation of resting $[K^+]_e$ in the extracellular space.

Different Subtypes of Astrocytes in the Gliotic Cortex

Similar to our findings, D'Ambrosio et al. (1999) also recognized three electrophysiologically different subtypes of reactive astrocytes: complex, inwardly rectifying, and linear (passive) astrocytes; however, these investigators did not describe astrocytes with upregulated K_{DR} currents. In agreement with our findings, Bordey et al. (2000, 2001) showed the enhanced expression of K_{DR} channels after a focal cortical freeze lesion. Astrocytes displaying K_{DR}, K_A, K_{IR}, and Na^+ currents were previously reported in other studies (Bordey and Sontheimer, 2000; MacFarlane and Sontheimer, 1997) as well. These data indicate that three electrophysiologically different types of astrocytes are present in the cortex, but we cannot exclude the presence of only a single, highly plastic type of astrocyte, as proposed by Walz (2000). The fact that the number of astrocytes displaying a prominent inward K^+ rectifier in addition to passive conductance increases during development supports the presence of only one type of astrocyte with different membrane properties (Kressin et al., 1995). Conversely, the observation of astrocytes with contrasting glutamate responsiveness in the hippocampus (Seifert et al., 1997; Bergles and Jahr, 1997, 1998; Zhou and Kimelberg, 2001) indicates the presence of distinct astrocyte cell types. In addition, independent populations of cells with astroglial properties displaying diverse morphological, molecular and functional patterns

have been demonstrated in the developing hippocampus (Matthias et al., 2003).

In contrast to our data, no changes in IR were reported in astrocytes from human epilepsy seizure foci (Bordey and Sontheimer, 1998) or in astrocytes after fluid percussion injury (D'Ambrosio et al., 1999), while our data showed that A2 astrocytes had significantly increased IR at both 3 and 7 days PI. There is evidence that passive K^+ currents are upregulated in astrocytes during postnatal maturation (Kressin et al., 1995); thus, the increase in IR might be related to the properties of glial precursors. In addition to IR changes, we observed a shift in V_m to more positive values in A1 astrocytes 3 days PI. The depolarization of astrocytes with K_{IR} currents was described previously (MacFarlane and Sontheimer, 1997; McKhann et al., 1997; Bordey and Sontheimer, 1998; Schröder et al., 1999). However, other studies have not reported any significant changes in V_m in astrocytes with K_{IR} currents (D'Ambrosio et al., 1999; Jabs et al., 1997).

Changes in Astrocyte Morphology Induced by a Cortical Stab Wound

The differences in the morphology of A2 and A1 astrocytes, expressed by the S/V ratio, confirmed the presence of two distinct types of astrocytes around the stab wound. A2 astrocytes, characterized by a low S/V ratio, were found only in the vicinity of the stab wound and displayed typical features of reactive astrocytes: hypertrophy, elevated GFAP expression and nestin and BrdU positivity. These astrocytes were proliferating and most likely derived from dedifferentiated GFAP-positive astrocytes, as proposed by Amat et al. (1996), or migrated to the site of the injury (Frisen et al., 1995). A1 astrocytes were characterized by the weak expression of GFAP, but still stronger than in controls, and they were never found in the vicinity of the stab wound. Based on the S/V ratio, A1 astrocytes underwent smaller changes in cell volume than did A2 astrocytes. This could imply either the presence of two functional subpopulations of astrocytes in cortical gray matter, distinguishable only under pathological conditions, or that A1 and A2 astrocytes are the same subclass of astrocytes, but in different stages of reactive gliosis. The presence of two subpopulations of reactive astrocytes has been proposed by many investigators (Malhotra et al., 1993; Ridet et al., 1996, 1997; Yang et al., 1997). In these studies, proximal reactive astrocytes, producing a permanent glia scar, were found in the immediate vicinity of a lesion, while distal reactive astrocytes were found farther from the destructive lesion and did not generate a permanent glia scar. The existence of three immunohistochemically distinct types of reactive astrocytes was demonstrated by Wang and Walz (2003).

Changes in the Expression of K_{IR} and K_{DR} Currents in Correlation With Resting $[K^+]_e$ and Proliferation

It is generally accepted that astrocytes participate in K^+ homeostasis in the CNS, mainly mediated by K_{IR} channels that have a high open probability near the astrocyte resting membrane potential (Roy and Sontheimer, 1995; Sontheimer, 1994). The increase in K_{IR} current densities of A1 and complex astrocytes within 1 day PI correlated with an increase in resting $[K^+]_e$ that lasted until the third day PI, while at 5 and 7 days PI, $[K^+]_e$ returned to control values. The increase in $[K^+]_e$ to 8–9 mM, measured in vivo within the first day PI, can be explained by increased neuronal excitability. It was also shown that disruption of the blood-brain barrier by stabbing the cortex most likely leads to ischemic conditions at the site of injury, resulting in neuronal dysfunction with hyperexcitability (Schiene et al., 1996) and to the downregulation of glial K_{IR} currents observed in the vicinity of the ischemic lesion (Koller et al., 2000). K^+ release from hyperactive post-traumatic neurons and the loss of Cs^+-sensitive K_{IR} currents in glia lead to K^+ accumulation in the hippocampus (D'Ambrosio et al., 1999). In contrast to data presented by D'Ambrosio et al. (1999) and Koller et al. (2000), and in agreement with data shown by Bordey et al. (2000), we found an upregulation of K_{IR} currents in post-traumatic A1 and complex astrocytes during the first day PI. In contrast to the reported reduction of K_{IR} currents (MacFarlane and Sontheimer, 1997; D'Ambrosio et al., 1999; Koller et al., 2000; Bordey et al., 2001), we did not observe any downregulation of K_{IR} currents in A1 astrocytes, but rather in complex astrocytes, 7 days PI. These discrepancies in the expression of K_{IR} currents can be explained by the different measurement time-points after injury, by different in vitro conditions or by the nature of the injury used in the various experiments.

Our data show a decreasing number of A1 and complex astrocytes from third day PI and an increasing number of A2 astrocytes. MacFarlane and Sontheimer (1997) took the presence of K_{IR} currents as a hallmark of mature astrocytes. In agreement with our results, Bordey and Sontheimer (1998) reported a 75% reduction in astrocytes expressing K_{IR} currents in gliotic tissue from epilepsy seizure foci. The switch from K_{IR} to K_{DR} currents was described as a possible injury-induced recapitulation of immature glial properties in reactive astrocytes in vitro, which correlates with our observations (MacFarlane and Sontheimer, 1997).

Outwardly rectifying K^+ channels are thought to be involved in cell proliferation and in maintaining "auxiliary" V_m under pathological conditions when the cellular membrane is depolarized and K_{IR} channels are nonactive (Chung et al., 1998; Pannicke et al., 2000), and they contribute to V_m maintenance after changes in $[K^+]_e$ (Chvátal et al., 1997). Similarly to our results, an upregulation of K_{DR} currents in reactive astrocytes was shown in situ (Bordey et al., 2001) and in vitro

(MacFarlane and Sontheimer, 1997; Perillan et al., 1999, 2000), as well as their sensitivity to 4-AP and TEA chloride. In addition to work conducted by other investigators (MacFarlane and Sontheimer, 1997; Bordey et al., 2001), we have shown that the appearance of A2 astrocytes correlates with astrocyte proliferation only at the immediate site of a stab wound. Since the loss of K_{IR} currents described by D'Ambrosio et al. (1999) results in the failure of glial K^+ homeostasis, increased outward conductance in A2 astrocytes might also reflect the changes in K^+ spatial buffering. In contrast to A1 and complex astrocytes, the proportion of A2 astrocytes in our experiments gradually increased from 3 to 5 days PI. Similarly to other studies, we found a negligible number of astrocytes with K_{DR} currents in the cortex of control animals (Jabs et al., 1997; D'Ambrosio et al., 1999; Bordey et al., 2001). However, besides K_{DR} and K_{IR} currents, other current components, such as KCNK channels (Goldstein et al., 2001), described in cultured cortical astrocytes by Gnatecko et al. (2002) and Ferroni et al. (2003), might also contribute to the total outward or inward K^+ conductance in astrocytes under pathological conditions.

Changes in K^+ and Na^+ Current Amplitudes in Complex Astrocytes

A significant increase in K_{DR}, K_A, K_{IR}, and Na^+ current densities was found only 6 h PI, at the time of the maximal increase in resting $[K^+]_e$. In comparison to control astrocytes, K_{IR} current amplitude remained increased until the first day PI and significantly decreased 3 days PI, while K_{DR}, K_A, and Na^+ current amplitudes returned to their control values 1 day PI. Since outwardly rectifying currents have been suggested to be also involved in K^+ homeostasis (Verkhratsky and Steinhauser, 2000) and Na^+ channels have been proposed to maintain ATPase function in glia (Sontheimer et al., 1994), major changes in their amplitudes could be expected immediately after injury, when resting $[K^+]_e$ is increased. Our findings are in agreement with data reported by MacFarlane and Sontheimer (1997), using an in vitro model of injury. The authors described an increase in K_A, K_{DR} and Na^+ current amplitudes 4 h after injury, while at 1 day post-injury the amplitudes returned to control values. After fluid percussion injury, no changes were reported in cortical complex astrocytes, whereas hippocampal complex astrocytes showed a loss of K_{IR} and K_A currents (D'Ambrosio et al., 1999). In contrast to our data, gliosis induced by an intraperitoneal injection of kainic acid caused a complete loss of TTX-S Na^+ channels in complex astrocytes (Jabs et al., 1997).

The presence of two electrophysiologically, immunohistochemically, and morphologically distinct types of hypertrophied astrocytes, depending on their distance from a stab wound, raises questions about their origin as well as contribution to ionic homeostasis and/or regeneration. Further studies are needed to elucidate whether reactive astrocytes are derived from glial precursors or preexisting astrocytes and what are the functional consequences of their distance-dependent appearance at the site of injury.

ACKNOWLEDGMENTS

The authors dedicate this publication to our colleague, Tatiana Antonova, who died unexpectedly at the age of 31 years.

REFERENCES

Amat, JA, Ishiguro H, Nakamura K, Norton WT. 1996. Phenotypic diversity and kinetics of proliferating microglia and astrocytes following cortical stab wounds. Glia 16:368–382.

Bergles DE, Jahr CE. 1997. Synaptic activation of glutamate transporters in hippocampal astrocytes. Neuron 19:1297–1308.

Bergles DE, Jahr CE. 1998. Glial contribution to glutamate uptake at Schaffer collateral-commissural synapses in the hippocampus. J Neurosci 18:7709–7716.

Bevan S, Lindsay RM, Perkins MN, Raff MC. 1987. Voltage gated ionic channels in rat cultured astrocytes, reactive astrocytes and an astrocyte-oligodendrocyte progenitor cell. J Physiol 82:327–335.

Bignami A, Dahl D. 1977. Specificity of the glial fibrillary acidic protein for astroglia. J Histochem Cytochem 25:466–469.

Bordey A, Sontheimer H. 1997. Postnatal development of ionic currents in rat hippocampal astrocytes in situ. J Neurophysiol 78:461–477.

Bordey A, Sontheimer H. 1998. Properties of human glial cells associated with epileptic seizure foci. Epilepsy Res 32:286–303.

Bordey A, Sontheimer H. 2000. Ion channel expression by astrocytes in situ: comparison of different CNS regions. Glia 30:27–38.

Bordey A, Hablitz JJ, Sontheimer H. 2000. Reactive astrocytes show enhanced inwardly rectifying K^+ currents in situ. NeuroReport 11:3151–3155.

Bordey A, Lyons SA, Hablitz JJ, Sontheimer H. 2001. Electrophysiological characteristics of reactive astrocytes in experimental cortical dysplasia. J Neurophysiol 85:1719–1731.

Burnard DM, Crichton SA, MacVicar BA. 1990. Electrophysiological properties of reactive glial cells in the kainate-lesioned hippocampal slice. Brain Res 510:43–52.

Chung S, Joe E, Soh H, Lee MY, Bang HW. 1998. Delayed rectifier potassium currents induced in activated rat microglia set the resting membrane potential. Neurosci Lett 242:73–76.

Chvátal A, Pastor A, Mauch M, Syková E, Kettenmann H. 1995. Distinct populations of identified glial cells in the developing rat spinal cord slice: ion channel properties and cell morphology. Eur J Neurosci 7:129–142.

Chvátal A, Berger T, Vorisek I, Orkand RK, Kettenmann H, Syková E. 1997. Changes in glial K^+ currents with decreased extracellular volume in developing rat white matter. J Neurosci Res 49:98–106.

D'Ambrosio R, Maris DO, Grady MS, Winn HR, Janigro D. 1999. Impaired K^+ homeostasis and altered electrophysiological properties of post-traumatic hippocampal glia. J Neurosci 19:8152–8162.

Enclancher F, Perraud F, Faltin J, Labourdette G, Sensenbrenner M. 1990. Reactive astrogliosis after basic fibroblast growth factor (bFGF) injection in injured neonatal rat brain. Glia 3:502–509.

Ferroni S, Valente P, Caprini M, Nobile M, Schubert P, Rapisarda C. 2003. Arachidonic acid activates an open rectifier potassium channel in cultured rat cortical astrocytes. J Neurosci Res 72:363–372.

Frisen J, Johansson CB, Torok C, Risling M, Lendahl U. 1995. Rapid, widespread, and longlasting induction of nestin contributes to generation of glial scar tissue after CNS injury. J. Cell Biol 131:453–464.

Gnatenco C, Han J, Snyder AK, Kim D. 2002. Functional expression of TREK-2 K^+ channel in cultured rat brain astrocytes. Brain Res 931:56–67.

Goldstein SA, Boskenhauer D, O'Kelly I, Zilberberg N. 2001. Potassium leak channels and the KCNK family of two-P-domain subunits. Nat Rev Neurosci 2:175–184.

Hamill OP, Marty A, Neher E, Sakmann B, Sigworth FJ. 1981. Improved patch-clamp techniques for high-resolution current record-

ing from cells and cell-free membrane patches. Pflugers Arch 391: 85–100.
Hinterkeuser S, Schroder W, Hager G, Seifert G, Blumcke I, Elger CE, Schramm J, Steinhauser C. 2000. Astrocytes in the hippocampus of patients with temporal lobe epilepsy display changes in potassium conductances. Eur J Neurosci 12:2087–2096.
Hozumi I, Aquino DA, Norton WT. 1990. GFAP mRNA levels following stab wounds in rat brain. Brain Res 534:291–294.
Jabs R, Paterson IA, Walz W. 1997. Qualitative analysis of membrane currents in glial cells from normal and gliotic tissue in situ: down-regulation of Na^+ current and lack of P2 purinergic responses. Neuroscience 81:847–860.
Kálmán M, Ajtai BM. 2000. Lesions do not provoke GFAP-expression in the GFAP-immunonegative areas of the teleost brain. Ann Anat 182:459–463.
Koller H, Schroeter M, Jander S, Stoll G, Siebler M. 2000. Time course of inwardly rectifying K^+ current reduction in glial cells surrounding ischemic brain lesions. Brain Res 872:194–198.
Kressin K, Kuprijanova E, Jabs R, Seifert G, Steinhäuser C. 1995. Developmental regulation of Na^+ and K^+ conductances in glial cells of mouse hippocampal brain slices. Glia 15:173–187.
MacFarlane SN, Sontheimer H. 1997. Electrophysiological changes that accompany reactive gliosis in vitro. J Neurosci 17:7316–7329.
MacFarlane SN, Sontheimer H. 1998. Spinal cord astrocytes display a switch from TTX-sensitive to TTX-resistant sodium currents after injury-induced gliosis in vitro. J Neurophysiol 79:2222–2226.
Malhotra SK, Svensson M, Aldskogius H, Bhatnagar R, Das GD, Shnitka TK. 1993. Diversity among reactive astrocytes: proximal reactive astrocytes in lacerated spinal cord preferentially react with monoclonal antibody J1–31. Brain Res Bull 30:395–404.
Matthias K, Kirchhof F, Seifert G, Huttmann K, Matyash M, Kettenmann H, Steinhäuser CH. 2003. Segregated expression of AMPA-type glutamate receptors and glutamate transporters defines distinct astrocytes populations in the mouse hippocampus. J Neurosci 23:1750–1758.
McKhann GM, D'Ambrosio R, Janigro D. 1997. Heterogeneity of astrocyte resting membrane potentials and intercellular coupling revealed by whole-cell and gramicidin-perforated patch recordings from cultured neocortical and hippocampal slice astrocytes. J. Neurosci 17:6850–6863.
Nolte C, Matyash M, Pivneva T, Schipke CG, Ohlemeyer C, Hanisch UK, Kirchhoff F, Kettenmann H. 2001. GFAP promoter-controlled EGFP-expressing transgenic mice: a tool to visualize astrocytes and astrogliosis in living brain tissue. Glia 33:72–86.
Norton WT. 1999. Cell reactions following acute brain injury: a review. Neurochem Res 24:213–218.
Pannicke T, Faude F, Reichenbach A, Reichelt W. 2000. A function of delayed rectifier potassium channels in glial cells: maintenance of an auxiliary membrane potential under pathological conditions. Brain Res 862:187–193.
Pastor A, Chvátal A, Syková E, Kettenmann H. 1995. Glycine- and GABA-activated current in identified glial cells of the developing rat spinal cord slices. Eur J Neurosci 7:1188–1198.
Perillan PR, Li X, Simard JM. 1999. K^+ inward rectifier currents in reactive astrocytes from adult rat brain. Glia 27:213–225.
Perillan PR, Li X, Potts EA, Chen M, Bredt DS, Simard JM. 2000. Inward rectifier K^+ channel Kir2.3 (IRK3) in reactive astrocytes from adult rat brain. Glia 31:181–192.
Ridet JL, Alonso G, Chauvet N, Chapron J, Koenig J, Privat A. 1996. Immunocytochemical characterization of a new marker of fibrous and reactive astrocytes. Cell Tissue Res 283:39–49.
Ridet JL, Malhotra SK, Privat A, Gage FH. 1997. Reactive astrocytes: cellular and molecular cues to biological function. Trends Neurosci 20:570–577.
Roitbak T, Syková E. 1999. Diffusion barriers evoked in the rat cortex by reactive astrogliosis. Glia 28:40–48.
Roy ML, Sontheimer H. 1995. Beta-adrenergic modulation of glial inwardly rectifying potassium channels. J Neurochem 64:1576–1584.
Schiene K, Bruehl C, Zilles K, Qu M, Hagemann G, Kraemer M, Witte OW. 1996. Neuronal hyperexcitability and reduction of GABAA-receptor expression in the surround of cerebral photothrombosis. J Cereb Blood Flow Metab 16:906–14.
Schröder W, Hager G, Kouprijanova E, Weber M, Schmitt AB, Seifert G, Steinhäuser C. 1999. Lesion-induced changes of electrophysiological properties in astrocytes of the rat dentate gyrus. Glia 28: 166–174.
Schröder W, Hinterkeuser S, Seifert G, Schramm J, Jabs R, Wilkin GP, Steinhäuser C. 2000. Functional and molecular properties of human astrocytes in acute hippocampal slices obtained from patients with temporal lobe epilepsy. Epilepsia 41:S181–184.
Seifert G, Zhou M, Steinhauser C. 1997. Analysis of AMPA receptor properties during postnatal development of mouse hippocampal astrocytes. J Neurophysiol 78:2916–2923.
Sontheimer H. 1994. Voltage-dependent ion channels in glial cells. Glia 11:156–172.
Sontheimer H, Fernandez-Marques E, Ullrich N, Pappas CA, Waxman SG. 1994. Astrocyte Na^+ channels are required for maintenance of Na^+/K^+-ATPase activity. J Neurosci 14:2464–2475.
Syková E. 1997. Extracellular space volume and geometry of the rat brain after ischemia and central injury. Adv Neurol 73:121–135.
Syková E, Chvátal A. 2000. Glial cells and volume transmission in the CNS. Neurochem Int 36:397–409.
Syková E, Svoboda J, Polak J, Chvátal A. 1994. Extracellular volume fraction and diffusion characteristics during progressive ischemia and terminal anoxia in the spinal cord of the rat. J Cereb Blood Flow Metab 14:301–311.
Verkhratsky A, Steinhauser C. 2000. Ion channels in glial cells. Brain Res Brain Res Rev 32:380–412.
Vijayan VK, Lee YL, Eng LF. 1990. Increase in glial fibrillary acidic protein following neural trauma. Mol Chem Neuropathol 13:107–118.
Walz W. 2000. Controversy surrounding the existence of discrete functional classes of astrocytes in adult gray matter. Glia 31:95–103.
Wang K, Walz W. 2003. Unusual topographical pattern of proximal astrogliosis around a cortical devascularizing lesion. J Neurosci Res 73:497–506.
Westenbroek RE, Bausch SB, Lin RC, Franck JE, Noebels JL, Catterall WA. 1998. Upregulation of L-type Ca2+ channels in reactive astrocytes after brain injury, hypomyelination, and ischemia. J Neurosci 18:2321–34.
Yang HY, Lieska N, Kriho V, Wu CM, Pappas GD. 1997. A subpopulation of reactive astrocytes at the immediate site of cerebral cortical injury. Exp Neurol 146:199–205.
Zhou M, Kimelberg HK. 2001. Freshly isolated hippocampal CA1 astrocytes comprise two populations differing in glutamate transporters and AMPA receptor expression. J Neurosci 21:7901–7908.